Acta Astronautica ▮ (▮▮▮▮) ▮▮▮–▮▮▮

Contents lists available at SciVerse ScienceDirect

Acta Astronautica

journal homepage: www.elsevier.com/locate/actaastro

Characterization of HTPB-based solid fuel formulations: Performance, mechanical properties, and pollution

L.T. DeLuca*, L. Galfetti, F. Maggi, G. Colombo, L. Merotto, M. Boiocchi, C. Paravan, A. Reina, P. Tadini, L. Fanton

SPLab, Aerospace Engineering Department, Politecnico di Milano, 34 Via La Masa, 20156 Milan, Italy

ARTICLE INFO

Article history:
Received 28 February 2012
Received in revised form
30 April 2012
Accepted 3 May 2012

Keywords:
Hybrid rocket propulsion
HTPB
Regression rate
Mechanical properties
Thermochemistry
Soot

ABSTRACT

Features such as safety, low-cost, and throttleability make hybrid rocket engines an attractive option for suborbital flights and space exploration missions in general. While the domain of possible liquid oxidizers is well characterized, the choice of a suitable solid fuel is still a matter of investigation. Space Propulsion Laboratory (SPLab) at Politecnico di Milano has developed a series of proprietary techniques to evaluate, on a relative grading, the quality of innovative solid fuels while visualizing at the same time their flame structure. But a serious alert was recently notified that soot emission from hydrocarbon fuels has the potential to contribute to global climate change. In this paper, HTPB polymer has been taken as baseline and characterized at laboratory level in terms of ballistic properties, mechanical testing, and thermochemical calculations.

1. Background

The perspective of space launch activities is presumably changing within few years. Past and current activities are mostly hold by governmental institutions but space tourism on one hand and the uncertainties related to future USA space manned missions (after Space Shuttle retirement) on the other, strengthen the position of private firms (such as Virgin Galactic, Xcor, Armadillo Aerospace, Blue Origin, Dassault, and others). As of now, suborbital flights for tourism and scientific research are likely to represent the major part of this market in the near and medium term future. Indeed several projects are currently under development, looking at the possibility to share a demand of about one thousand launches per year, once the market is fully developed [1].

Space tourism was started by Mr. Dennis Tito ten years ago, with an orbital mission combining Soyuz TM-32, ISS-EP1, and Soyuz-TM-31 for almost 8 days at $20 million in April 2001. Since then it has extended to suborbital flights: SpaceShipOne by Mojave Aerospace Ventures won the Ansari X Prize of $10 million in October 2004. Meanwhile a range of appealing new projects materialized, including lunar flyby tours (Space Adventures, two seats per flight offered at $150 million each), space stations (Space Adventures selling flights to ISS for $20 million/passenger and the recent Excalibur Almaz by Jurby), space hotels (Bigelow Aerospace), and so on. In particular, suborbital space tourism is expected to be a $700 million industry by 2020, flying thousands of passengers a year to the near zero gravity of the outer space edge. Projects are being developed not only in USA but also by Dassault, EADS Astrium, and Project Enterprise (Black Sky spaceplane) in Europe; other initiatives were notably triggered in Russia and Japan. Overall, private human access to space represents an incredible opportunity for aerospace industry.

* Corresponding author.
E-mail addresses: luigi.deluca@tiscali.it, luigi.deluca@polimi.it (L.T. DeLuca).

0094-5765/$ - see front matter © 2012 Elsevier Ltd. All rights reserved.
http://dx.doi.org/10.1016/j.actaastro.2012.05.002

The most ambitious project is SpaceShipTwo by Virgin Galactic, whose objective is to realize a massive program of commercial suborbital flights to paying passengers (space tourism) by running a world-wide fleet of vehicles. Each spaceship (one hybrid rocket engine) will run twice a day while the carrier plane (four jet engines) will run up to four times a day. For each flight SpaceShipTwo will accommodate two pilots and six passengers at $200,000 per seat. By reaching 110 km altitude, the passengers will enjoy about 5 min of reduced gravity. Within few years, a total of 50 carrier planes are expected to be operated for space tourism, orbit injection of small satellites, and more.

Hybrid rocket propulsion is a good candidate for the above kind of applications, being safer and more performing than solid propellants in terms of gravimetric specific impulse, less expensive than liquid propellants in terms of development and management of the propulsive system, and (at least claimed to be) environmentally-friendly. Mainly for its intrinsic safety and low-cost features, hybrid rocket propulsion is specially suited for private human access to space. For hybrid rocket propulsion, the option is available to select the best ingredients already known from liquid and solid rocket propulsion. The choice of liquid oxidizer heavily affects the whole propulsive system design, but the related technology is well characterized thanks to the huge expertise collected during last decades from liquid rocket propulsion. On the contrary, solid fuel technology for hybrid propulsion still requires improvements. Limitations are indeed still faced, such as low regression rate and combustion inefficiency, causing unproven capability of large rocket operations. Overall, the low readiness level of hybrid propulsion, evaluated between 2 and 3 for large-scale engines, is still a significant drawback. Therefore, intense research activities are currently ongoing in this field [2].

The current work presents a complete laboratory investigation on solid fuels based on the HTPB polymer (taken as a nonmetallized baseline). Although paraffin-based solid fuels allow much larger regression rates (with the penalty of poor mechanical properties), HTPB or other polymers are commonly used in several projects: HTPB/N_2O in Mojave Aerospace Ventures SpaceShipOne, again HTPB/N_2O in Virgin Galactic SpaceShipTwo, HTPBc (containing a small amount of some unspecified particle fillers)/87.5% H_2O_2 in Nammo, epoxy/N_2O in Copenhagen Suborbitals HATV or polyurethane/LOX in Copenhagen Suborbitals HEAT, etc. Thermochemical analyses suggest that HTPB binder can profitably be used as a solid fuel in hybrid rockets, granting higher specific impulse with respect to solid propulsion. Nevertheless, the realization of expected performance enhancement requires the knowledge of all interleaving phenomena occurring during the combustion and, thus, a full characterization is required.

Ballistic and mechanical properties will be presented and critically analyzed. Moreover, considering the discussions triggered by a recent paper by Ross et al. [3] on hybrid rocket environmental impact, an analysis of pollutant emissions will be conducted through calculations made under ideal assumptions. Focus will primarily be posed on carbon black as the responsible of potential climate changes, while considering four different potential oxidizers in the perspective of small-scale motor testing for real applications in the field of space tourism.

2. Experimental ballistics

Two hybrid burners were designed to enable relative ballistic grading of different fuel formulations and are currently in use at SPLab: a 2D radial setup suitable for time-resolved quasi-steady ballistics and a 2D slab setup suitable for boundary layer analyses and flow field visualization.

The simple SPLab 2D radial burner enables a continuous tracking of the solid fuel gasifying surface during test at the visible sample cross-section. Therefore, for the visualized section, time-resolved regression rate can be achieved with a simple and low-cost experimental setup.

Several tests for HTPB fuel burning in GOx were investigated to assess the quality of the proposed technique, even under transient conditions. Fuel was prepared starting from HTPB R45 resin cured by IPDI, using DOA as plasticizer and Dibutyltin Diacetate as curing catalyst. A degas cycle of the fuel formulation before molding of the samples grants realization of strands with high quality and porosity lower than 1%.

The main task is to experimentally identify a solid fuel formulation featuring adequate steady regression rates and short settling times in case of transient operations. In this framework, SPLab has developed a series of proprietary techniques to evaluate the quasi-steady ballistics of solid fuels, including regression rates, while visualizing at the same time their flame structure.

2.1. Experimental facility: 2D-radial burner

A schematic overview of the implemented 2D-radial (micro) burner is shown in Fig. 1. The combustion chamber is a stainless steel cylinder housing the injector head and optical accesses for test visualization. The main observable of interest is the regression rate of the single perforation cylindrical solid fuel sample. During combustion the burning cross-section of the tested fuel is fully visible thanks to a proper combination of lateral windows and a 45 degree mirror placed inside the combustion chamber. The regression rate can therefore be monitored by an optical technique tracking the gasifying surface history of the fuel grain all along the combustion process [4–7].

Both oxidizer mass flow and chamber pressure of the test rig can be regulated independently, thus allowing different test conditions to be easily explored.

The oxidizer is fed by cylinders and is injected through a number of holes realized in the internal surface of the sample holder, thus providing control on the nature of the flow investing the fuel sample. Both axial and swirled oxidizer flowing over the tested fuel surface can be achieved; the latter is commonly employed. The oxidizer is delivered to the injector by a dedicated primary feed line instrumented with measuring and controlling hardware for the mass flowing through the central port and

Please cite this article as: L.T. DeLuca, et al., Characterization of HTPB-based solid fuel formulations: Performance, mechanical properties, and pollution, Acta Astronautica (2012), http://dx.doi.org/10.1016/j.actaastro.2012.05.002

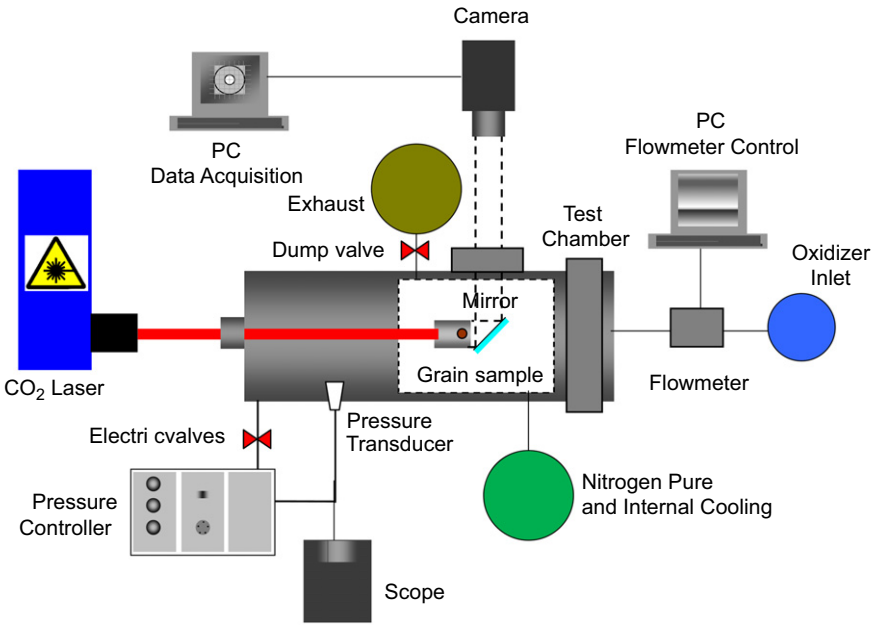

Fig. 1. 2D-radial burner facility overview.

taking part in the combustion process. The oxidizer flow is measured by a mass flowmeter and regulated by a needle valve. A secondary feed line enables a Nitrogen flow to cool the chamber walls and prevent soot deposition hindering the burning process visualization. A switch allows using the secondary flow also as a purge to stop combustion.

A dump pipeline connecting the combustion chamber to servovalves grants a controlled pressure level during combustion. Servoactuators are characterized by a response time of 4 to 16 ms, and were driven by a regulator receiving signals from a piezoresistive pressure transducer (pressure range up to 70 bar and maximum error 0.1% full scale) placed in the combustion chamber. The instantaneous pressure and photodiode signals are finally sent to an oscilloscope, thus enabling detailed test analyses.

Sample ignition is achieved by a pyrotechnic primer charge, inserted in the central port of the solid fuel grain and in turn ignited by a CO_2 laser beam impinging on it. The overall combustion process is recorded by a range of video-cameras operated at different speeds, up to 10,000 fps, depending on the expected fuel regression rate. The video signal, after passing through a timing device, is digitalized by a computer where all raw data are collected and stored.

2.2. Time-resolved regression rate

Visualization of the sample cross-section during combustion enables continuous tracking of the solid fuel surface while regressing; see Fig. 2. For each test, a reference starting time ($t=t_0$) was set as the instant at which the laser beam starts impinging on the primer charge, whose combustion in turn ignites the solid fuel under test. To avoid the difficulties of the observed transient burning regime, the investigated measurement range started when the central port first appeared fully inflamed. As shown in Fig. 2, the 2D-radial burner enabled a complete vision of the sample cross-section during the subsequent quasi-steady burning regime. Thanks to this feature, regression rates could be evaluated along different radial directions, therefore achieving a complete characterization of combustion evolution in time at the visible cross-section.

Starting from the recorded video of a test, an average diameter $\overline{D}_i$ of the sample central port is defined for each i-th sampling time. The regression is computed starting from an initial diameter, denoted as ignition diameter $\overline{D}_{ign}$, corresponding to the diameter for which the central port first appears completely ignited by the primer charge. The collected succession of sampled mean diameters $\overline{D}_i$ is then interpolated by a power law, describing the evolution in time of the instantaneous mean diameter $\overline{D}(t)$ with respect to its nominal initial value D_0 at starting ($t=t_0$), as shown in Eq. (1).

$$\overline{D}(t)-D_0 = a_D(t-t_0)^{n_D}, \quad t \geq t_{ign} > t_0 \tag{1}$$

The ignition time, t_{ign}, is needed to avoid the singularity at $t=t_0$ and is defined ad-hoc as the one maximizing the data fitting according to the power law assumed in Eq. (1). The obtained value of t_{ign} is verified by a convective ignition delay model [8] as shown in Figs. 3 and 4.

Once the quasi-steady history $\overline{D}(t) - D_0$ of the central port diameter in time is obtained, all of the ballistic parameters of interest can be evaluated. In particular, the regression rate can easily be defined according to Eq. (2) by differentiating the above power law. Thus, an analytical description of the quasi-steady regression rate time dependence of the central port diameter follows as:

$$r_f(t) = \frac{1}{2}\frac{d[\overline{D}(t)-D_0]}{dt} = \frac{1}{2}a_D n_D (t-t_0)^{n_D-1}, \quad t \geq t_{ign} > t_0 \tag{2}$$

Please cite this article as: L.T. DeLuca, et al., Characterization of HTPB-based solid fuel formulations: Performance, mechanical properties, and pollution, Acta Astronautica (2012), http://dx.doi.org/10.1016/j.actaastro.2012.05.002

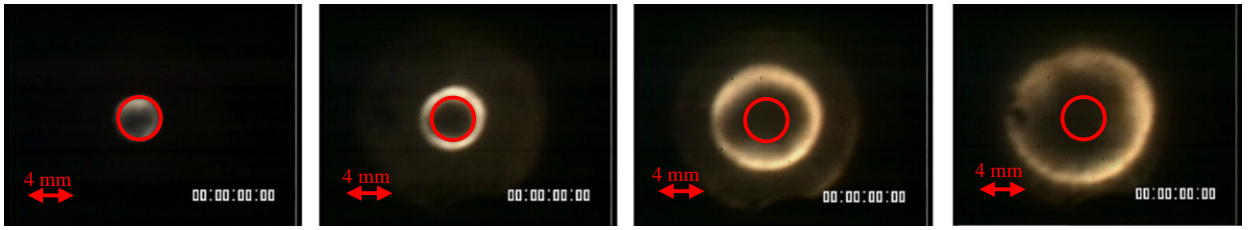

$t = t_{ign}$ $t = t_{ign} + 0.8s$ $t = t_{ign} + 4s$ $t = t_{ign} + 7.8s$

Fig. 2. Regressing surface evolution in time for HTPB burning under GOX. Operating conditions: initial oxidizer mass flux ~130 kg/(m^{2}s), chamber pressure 10 bar. Red circle marks the initial port diameter (4 mm). (For interpretation of the references to color in this figure legend, the reader is referred to the web version of this article.)

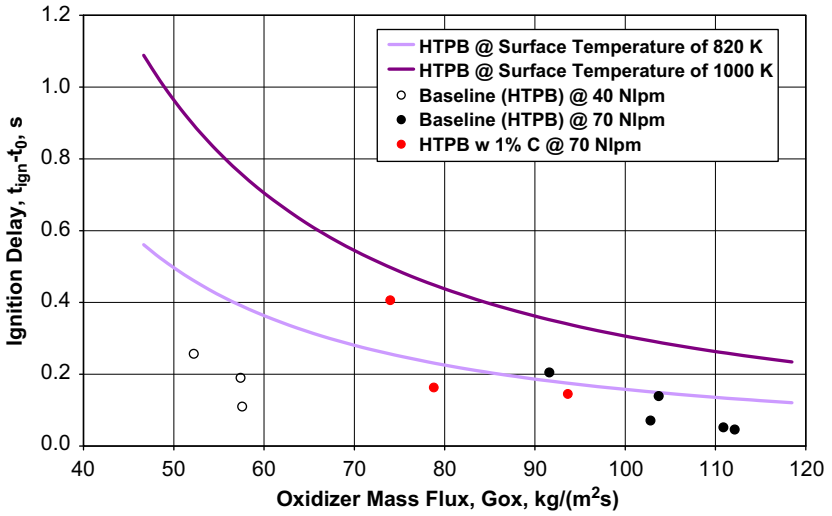

Fig. 3. Convective ignition delay values for t_{ign}: tests performed at 10 bar compared to predictions from [8] based on two different surface temperatures values [9,10]. Convective heat transfer coefficient evaluated by Gnielinski formula [11].

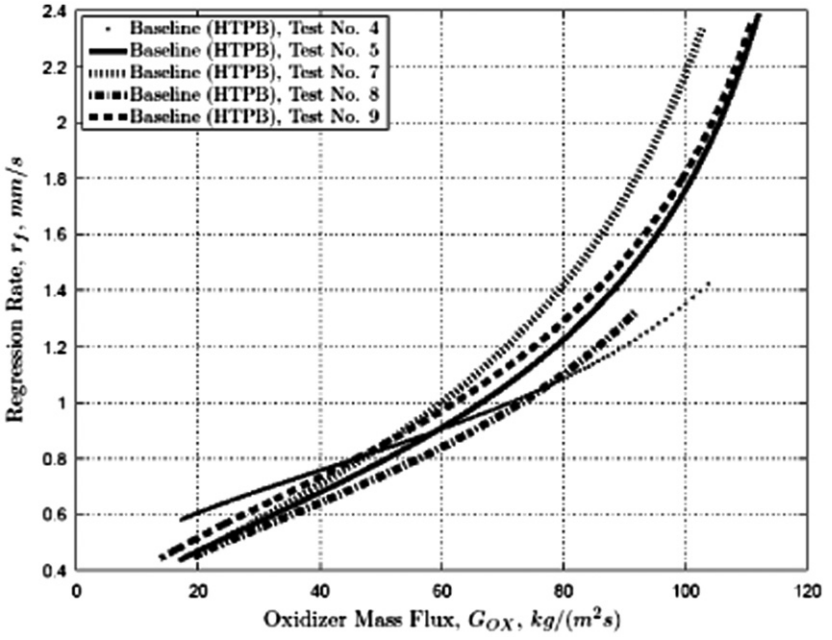

Fig. 4. Instantaneous regression rate values of HTPB burning in GOX, Operating conditions: initial oxidizer mass flux of ~130 kg/m^{2}s, chamber pressure 10 bar.

Please cite this article as: L.T. DeLuca, et al., Characterization of HTPB-based solid fuel formulations: Performance, mechanical properties, and pollution, Acta Astronautica (2012), http://dx.doi.org/10.1016/j.actaastro.2012.05.002

Similarly, the oxidizer mass flux G_{ox}, fuel mass flow rate m_f, and oxidizer-to-fuel ratio O/F, can easily be evaluated. Also, the average values of all quantities over the time span $\Delta t = t_b - t_{ign}$ can immediately be assessed. For example, at any arbitrary $t_b = t \geq t_{ign} > t_0$, one finds for the average regression rate

$$< r_f(t - t_{ign}) > = \frac{\int_{t_{ign}}^{t} [r_f(t)]dt}{t - t_{ign}} = \frac{a_D n_D}{2} \frac{\int_{t_{ign}}^{t} (t - t_0)^{n-1} dt}{t - t_{ign}} \quad (3)$$

This is an exact value if no additional effects (for example, axial contribution to burning or fuel fragmentation) come into play

For the investigated operating conditions and implemented optical hardware, the most suitable sampling frequency depends on the expected regression rate. For the implemented steady-state operating conditions, sufficient accuracy is found in the range 3–10 Hz; higher sampling rates were used for transient regression phenomena.

In most cases, regression rates are given by experimentalists as average values in time and/or space under a given set of operating conditions. This is a convenient procedure, but potentially misleading since, differently than burning rates of interest in solid propulsion, regression rates in hybrid propulsion are in principle both time- and space-dependent. At the very least, regression rate data should always be accompanied by precise information about the measurement technique and the enforced averaging procedure, together with the associated error band assessment.

An alternative approach is to deduce the average regression rate, over each sampled time interval $t_{i+1} - t_i$, directly from the raw diameter data as a TOT (Thickness-Over-Time) ratio of sampled diameter difference over sampled time difference during combustion

$$\overline{r}_{f,i+1/2} = \frac{1}{2} \frac{\overline{D}_{i+1} - \overline{D}_i}{t_{i+1} - t_i} \quad (4)$$

This TOT discrete measurement technique, often used in literature, quickly and easily provides a discrete set of data $\overline{r}_{f,i+1/2}$ which, however, is intrinsically prone to larger errors since based on raw data handling prior to smoothing. Notice that no analysis of the ignition transient is required.

All collected data are checked by appropriate mathematical expressions to verify congruence of the implemented measurement techniques. Congruence checks include the regression rate $r_f(t_{ign})$ at ignition, the average regression rate $\langle r_f(t) \rangle$ evaluation and the average oxidizer flux $\langle G_{ox}(t) \rangle$ evaluation. A detailed description of the ballistic parameters derivation and congruence relationships is reported in [7].

In order to have an easier comparison with the many datasets available in the literature, a standard power-law approximation of regression rate vs. oxidizer mass flux is considered, for each test and for the resulting ensemble curve, as

$$r_f(G_{ox}) = a_r \cdot G_{ox}(t)^{n_r}, \quad t \geq t_{ign} > t_0 \quad (5)$$

2.3. Representative results of time-resolved solid fuel burning

Pure HTPB was examined as a reference baseline, in consideration of its wide use in the current suborbital systems and because of its excellent mechanical properties. Operating conditions for combustion tests include chamber pressure ranging from 7 to 13 bar, burning in Gaseous Oxygen (GOX), with oxidizer volumetric flow rates of 40 Nlpm and 70 Nlpm corresponding to initial oxidizer mass fluxes of ~80 and ~130 kg/m^{2}s for a sample initial port diameter (D_0) of 4 mm.

Due to the initial curl, the standard power-law fitting of the regression rate in the oxidizer mass flux does not properly match the instantaneous data [12]. See Table 1 for time-resolved regression rate analysis and Table 2 for the corresponding TOT analysis; data congruence is tested in Table 3. In spite of the scattered single regression rate tests, in Table 1 the resulting instantaneous ensemble curve exhibits a reassuring slope ($n = 0.784$) quite close to

Table 2
Ballistic coefficients and data fitting (R^2) for TOT regression technique. Operating conditions: initial oxidizer mass flux ~130 kg/(m^{2}s), chamber pressure 10 bar.

Fuel formulation (Test no.)	Regression rate, r_f, mm/s		
	Thickness Over Time (TOT)		
	a_r	n_r	R^2
Baseline (04)	0.097 ± 0.034	0.559 ± 0.096	0.86
Baseline (05)	0.061 ± 0.040	0.676 ± 0.186	0.82
Baseline (07)	0.034 ± 0.006	0.834 ± 0.045	0.99
Baseline (08)	0.047 ± 0.015	0.713 ± 0.087	0.94
Baseline (09)	0.091 ± 0.024	0.581 ± 0.080	0.95

Table 1
Ballistic coefficients and data fitting (R^2) for time-resolved regression technique. Operating conditions: initial oxidizer mass flux ~130 kg/(m^{2}s), chamber pressure 10 bar.

Fuel formulation (Test no.)	Regression rate, r_f, mm/s					
	Instantaneous			Time-average		
	a_r	n_r	R^2	a_r	n_r	R^2
Baseline (04)	0.129 ± 0.006	0.489 ± 0.011	0.96	0.014 ± 0.001	0.615 ± 0.011	0.98
Baseline (05)	0.031 ± 0.003	0.854 ± 0.023	0.94	0.014 ± 0.001	1.051 ± 0.023	1.00
Baseline (07)	0.022 ± 0.002	0.954 ± 0.022	0.96	0.010 ± 0.001	1.137 ± 0.022	0.98
Baseline (08)	0.053 ± 0.003	0.685 ± 0.014	0.97	0.031 ± 0.002	0.814 ± 0.013	0.99
Baseline (09)	0.044 ± 0.004	0.783 ± 0.021	0.94	0.021 ± 0.002	0.961 ± 0.021	0.96
Ensemble (04–09)	0.042 ± 0.004	0.784 ± 0.021	0.93	0.019 ± 0.002	0.978 ± 0.022	0.96

Please cite this article as: L.T. DeLuca, et al., Characterization of HTPB-based solid fuel formulations: Performance, mechanical properties, and pollution, Acta Astronautica (2012), http://dx.doi.org/10.1016/j.actaastro.2012.05.002

the theoretical prediction of 0.8 for pure diffusion-limited models of boundary-layer turbulent combustion [13]. Notice on the other hand the larger values of slope for the corresponding single time-average curves; thus, the resulting time-average ensemble curve exhibits a slope ($n=0.978$) above the theoretical expectation.

Additional tests were conducted with HTPB loaded with 1% C and showed no significant changes with respect to the baseline formulation: $n=0.688$ (instead of 0.784) and a slightly increased regression rate, as illustrated in the ensemble plot of Fig. 5.

Further tests were conducted under different chamber pressures and revealed no significant pressure dependence of regression rate for pure HTPB, in contrast with a weak negative dependence for other formulations of interest, over the investigated experimental range of 4 to 16 bar [14].

Table 3
Results for data congruence of regression techniques. Operating conditions: initial oxidizer mass flux ~130 kg/(m^{2}s), chamber pressure 10 bar.

Fuel formulation (Test no.)	Regression data congruence: instantaneous vs. TOT data, % difference		
	Ignition rate, $r_f(t_{ign})$	Average rate, $<r_f>$	Average flux, $<G_{Ox}>$
Baseline (04)	−0.4	+4.6	+4.8
Baseline (05)	−0.2	+0.7	−1.4
Baseline (07)	+0.0	+1.2	−2.3
Baseline (08)	−0.2	+2.7	+0.6
Baseline (09)	+0.0	−0.1	+4.0

2.4. Exploratory tests on transient effects

A few exploratory tests were conducted to assess the feasibility of transient regression rate measurements. Changes of pressure or oxidizer mass flow rate were imposed and the subsequent effects on regression rate monitored. Visualization of the sample cross-section during combustion was performed using a Photron High-Speed Camera, with a recording frame rate of 250 fps and 750×750 pixel of resolution. While changes of pressure in the range 7–13 bar brought only minor effects, interruption of the oxidizer mass flow rate for 1 s revealed an interesting phenomenon of apparent extinction followed by reignition. Combustion ceased immediately after the oxidizer disruption; but when fresh oxidizer feeding was resumed, combustion restarted triggered by hot spots at the sample head-end and spread over the entire central port. Significant flame oscillations were visible during the reignition phase (see video sequence in Fig. 6, showing flame extinction in the above strip and spontaneous reignition in the bottom strip).

2.5. Experimental facility: 2D-slab burner

Further firing tests were performed using a 2D slab burner. The chamber is equipped with suitable oxygen and nitrogen inlet systems, a pressure transducer (*Repcom CTE7000*), a calibrated nozzle for the mass flow rate measurement. Nitrogen is used for a quick extinction of the oxidation reactions after the oxygen shut off. The combustion onset is achieved using a pyrotechnic igniter, consisting in about 1 g charge of solid propellant placed at the sample head-end. The solid propellant is in turn ignited by a hot Ni–Cr wire.

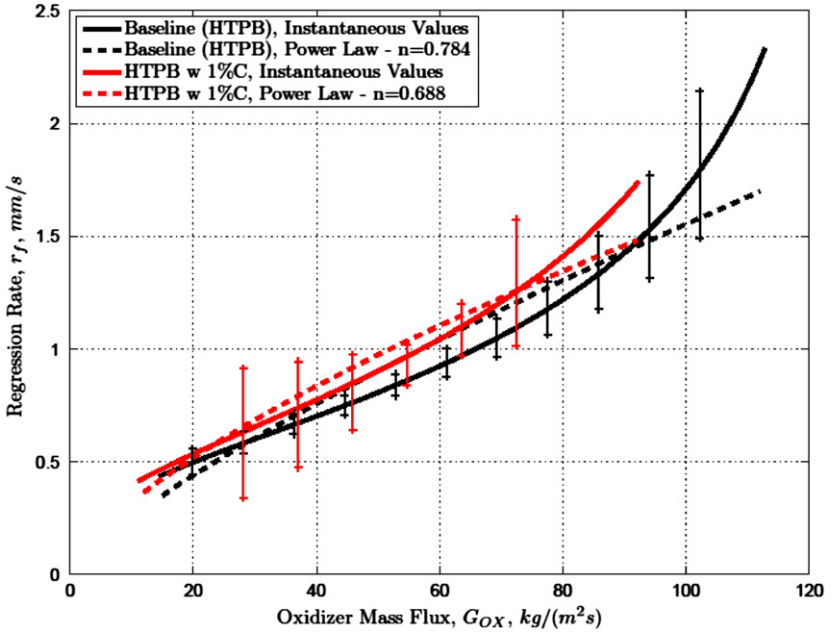

Fig. 5. Ensemble regression rate curves of HTPB (black) and HTPB with 1% C (red) burning in GOX. Operating conditions: initial oxidizer mass flux ~130 kg/(m^{2}s), chamber pressure 10 bar. (For interpretation of the references to colour in this figure legend, the reader is referred to the web version of this article.)

Please cite this article as: L.T. DeLuca, et al., Characterization of HTPB-based solid fuel formulations: Performance, mechanical properties, and pollution, Acta Astronautica (2012), http://dx.doi.org/10.1016/j.actaastro.2012.05.002

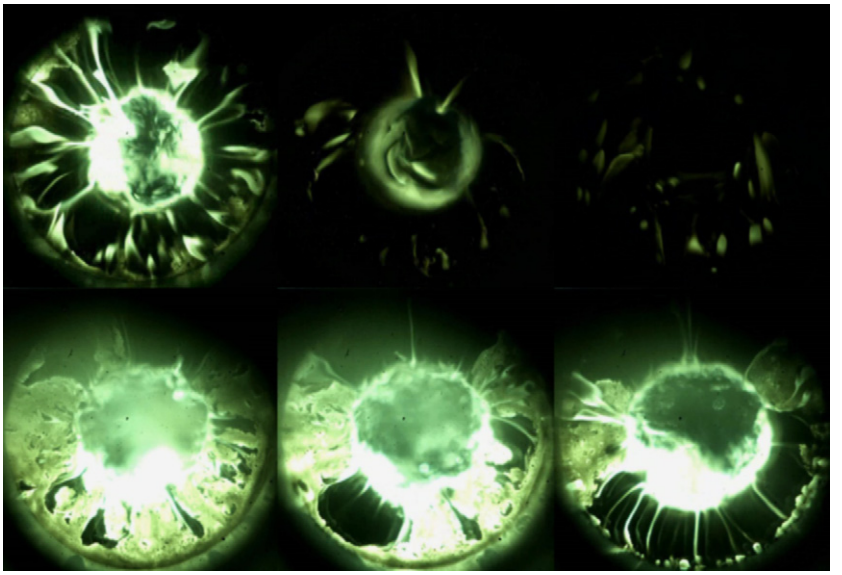

Fig. 6. Stop and restart combustion sequence following oxidizer mass flow disruption.

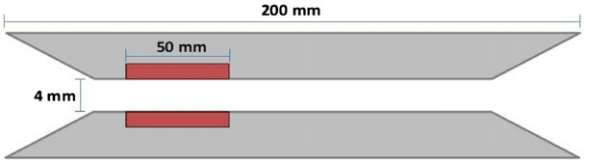

Fig. 7. Sample holders designed for this work showing the fuel slabs in red. (For interpretation of the references to colour in this figure legend, the reader is referred to the web version of this article.)

The sample holders designed for this work are shown in Fig. 7, with the fuel slabs (size: $50 \times 10 \times 4$ mm) drawn in red. A double slab configuration is used for the firing tests. The average regression rate (r_f) is measured from the burned mass (Δm, in the range 3–5 g depending on the slab configuration), the fuel density (ρ_f, equal to 0.93 g/cm^3 for pure HTPB, and 0.99 g/cm^3 for HTPB added with 10% nAl), the burning time (t_b, of the order of 6–7 s) and the burning area (A_b), using the following equation

$$r_f = \frac{\Delta m}{\rho_f t_b A_b} \tag{6}$$

A pure HTPB (no C) fuel formulation was used as baseline reference fuel. HTPB was investigated in pure and doped compositions; nAl powders (average size 0.05 and 0.1 μm) were used as fillers, at 10% mass fraction. Metal additives can raise the theoretical flame temperature, produce a strong radiation flux from the metal oxide combustion products, reduce the blocking effect of the blowing pyrolyzed mass. The time- and space-averaged regression rate was measured in two different configurations: the first was a one-slab, the second a two-slab configuration. In the one-slab, under the investigated operating conditions, the linear regression rate decreases. The effect of the upper cold wall does not allow combustion and energy release of nAl particles. The regression rate measurement for the double slab configuration results in a significant increase (up to 26%) as shown in Fig. 8.

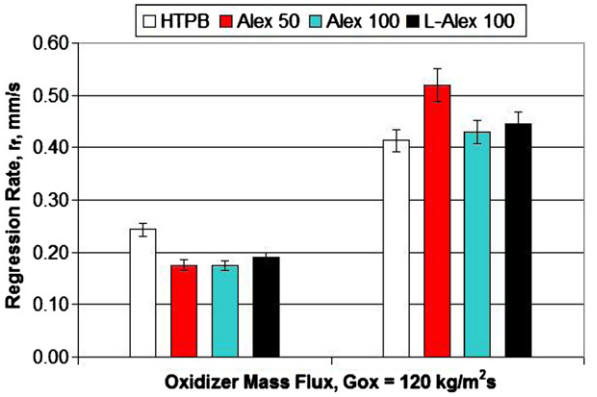

Fig. 8. Comparing average regression rates of HTPB-based fuels loaded with nAl powders. Single and double-slab configurations burning in GOX. Operating conditions: initial oxidizer mass flux 120 kg/(m^{2}s), chamber pressure 1.5 bar.

The average regression rate was estimated for the radial burner at the oxidizer flux of 120 kg/m^{2}s, under the three pressures of 7, 10 and 13 bar. Extrapolation to 1.5 bar provides an estimated regression rate for the radial burner of 0.74 mm/s. Under the same operating conditions, the measured regression rate in the slab burner, shows an average value of 0.41 mm/s. The ratio of the two regression rates ($r_{f,radial}/r_{f,slab} = 0.74/0.41 = 1.80$) shows a higher regression rate for the radial configuration.

The 2D radial burner aims to investigate the time-resolved regression rate. The aim of the tests performed in the slab burner is the investigation of the flame structure and the boundary layer behavior to understand details of the combustion processes in hybrid propulsion systems.

Please cite this article as: L.T. DeLuca, et al., Characterization of HTPB-based solid fuel formulations: Performance, mechanical properties, and pollution, Acta Astronautica (2012), http://dx.doi.org/10.1016/j.actaastro.2012.05.002

In particular, nano-aluminized compositions point out the role of the radiation heat-transfer to the solid fuel surface. The double slab configuration also allows highlighting the effects of nAl size. A comparison of Alex50 (size 0.05 μm) with Alex100 (size 0.10 μm) shows higher regression rate for the smaller powder, due to the higher rate of exothermic reactions in the boundary layer region close to the fuel surface. In double slab, nAl particles combustion and energy release, close to the fuel surface, provide a faster HTPB degradation and thus increase the regression rate.

The comparison of regression rate results in the slab burner with those obtained in the radial burner shows the important role of geometric effects. The initial cross-sectional area of the radial and slab fuel ports are approximately the same, being the initial diameter of the radial almost the same as the initial gap between the two fuel slabs. Nevertheless, tests show different regression rates, due to different internal flows, to problems linked to merging boundary layers, and to different effects of radiation in the two geometries. Moreover, the operating pressure ranges for the slab and the radial set up are not the same, due to experimental facilities restrictions concerning the slab device. Tests in slab geometry were performed at 1.5 bar chamber pressure, while radial tests were in the range 7–13 bar.

3. HTPB-based fuels mechanical properties

HTPB is a polymer widely used in propulsion both for solid propellants and hybrid fuels. This is due to the HTPB ease of manufacturing and capacity of providing good mechanical properties also to highly loaded grains. Here a mechanical characterization based on uniaxial tensile stress test is provided for the HTPB baseline formulation and HTPB loaded with 2% C.

Uniaxial tensile tests have been performed with an Instron Series 4302 with a load cell of 1kN and on "dog bone" samples following the standard DIN 53 504 S3A. A video recording system is used to monitor the test and compensate Instron crosshead data from sample slippage from the holders. By proper video measurement of the evolution of the distance between markers on the strand during test, the latter parameter can be related to specimen deformation, $\Delta L_{Specimen}$, as reported in Eq. (7) so that Instron rough output can be converted into measurement of sample elongation. The choice of a power law is dictated by best fitting motivations.

$$\Delta L_{Specimen} = a \cdot \Delta L_{Clamp}^{n} \tag{7}$$

Starting from Eq. (7), it is possible to define the linear strain (ε_{Lin}), according to Eq. (8)

$$\varepsilon_{Lin} = \Delta L_{Specimen} / L_{Specimen} \tag{8}$$

And, finally, logarithmic strain (ε_{Log}) and true stress (σ_{True}) can be defined with Eqs. (9 and 10) by considering linear strain and engineering stress (σ_{Eng}) that is the ratio of applied force to the initial, non-deformed cross sectional area of the specimen.

$$\varepsilon_{Log} = \ln(1+\varepsilon_{Lin}) \tag{9}$$

Table 4
Baseline formulation (HTPB): tangent Young's Modulus at 10% strain, mean value. Data scattering defined by standard deviation.

Batch no.	Tangent Young's modulus, $E_{tan,10\%}$, MPa
01 (Tests from no. 01 to no. 04)	1.40 ± 0.12
02 (Tests from no. 05 to no. 08)	1.26 ± 0.06
Tests no. 01 to no. 08	1.33 ± 0.12

Table 5
Baseline formulation (HTPB): true stress and logarithmic strain at break. Data scattering defined by standard deviation.

Batch no.	True stress at break, $\sigma_{True\ at\ break}$, MPa	Logarithmic strain at break, $\varepsilon_{Log\ at\ break}$
01 (Tests from no. 01 to no. 04)*	1.29 ± 0.03	0.74 ± 0.03
02 (Tests from no. 05 to no. 08)	1.24 ± 0.23	0.70 ± 0.08
Tests no. 01 to no. 08	1.25 ± 0.14	0.72 ± 0.05

* Test no. 01 was not considered in the analysis because breakage was influenced by clamp.

Table 6
HTPB loaded with 2% C: tangent Young's modulus at 10% strain - mean value – and its variation with respect to Baseline formulation. Data scattering defined by standard deviation, three tests performed for Carbon-loaded fuel.

	Tangent Young's modulus, $E_{tan,10\%}$, MPa
HTPB loaded with 2% C	1.45 ± 0.03
Difference wrt Baseline, % of $E_{\tan,10\%}^{Baseline}$	9.2%

Table 7
HTPB loaded with 2% C: true stress and logarithmic strain at break.

	True stress at break, $\sigma_{true\ at\ break}$, MPa	Logarithmic strain at break, $\varepsilon_{Log\ at\ break}$
HTPB loaded with 2% C *	1.34 ± 0.14	0.76 ± 0.03
Difference wrt Baseline, % of Baseline value	7.2%	5.0%

* Test No. 01 was not considered in this analysis because breakage was affected by clamp.

$$\sigma_{True} = \sigma_{Eng}(1+\varepsilon_{Lin}) \tag{10}$$

Experimental results of tensile tests performed with a crosshead speed of 50 mm/min are reported in Tables 4 and 5 for the baseline formulation and in Tables 6 and 7 for HTPB loaded with 2% C. Comparing achieved results for Baseline and Carbon-loaded formulation, the influence of filler on mechanical properties is apparent: loading polymeric matrix with Carbon enhance tangent elastic

Please cite this article as: L.T. DeLuca, et al., Characterization of HTPB-based solid fuel formulations: Performance, mechanical properties, and pollution, Acta Astronautica (2012), http://dx.doi.org/10.1016/j.actaastro.2012.05.002

modulus of around 9% with respect to baseline value, a typical result for filler loaded materials [15]. Due to good adhesion characteristics of Carbon, an active filler, also true stress and elongation at break of the loaded formulations result slightly higher than those of the baseline fuel.

4. Dispersion of nano-aluminum in HTPB

Metals and hydrides are often considered as additives, but with ambiguous results [16,17]. Fuels loaded with some materials, such as micrometric Aluminum (μAl), show even a decrease in regression rate, in particular for low mass flux. This behavior can be explained considering the high temperature required by Aluminum to ignite. Reducing particle size down to nanometric scale cause a great decrease in Aluminum ignition temperature, making the powder more reactive and the beneficial effect on regression rate more evident. Tests performed on HTPB loaded with different kind of nanometric Aluminum (nAl) can show good performance but with a low level of repeatability [18]: an explanation can be given considering the problem in obtaining samples with homogeneous dispersion of the nanometric powders. In fact it is very difficult to disperse nano-powders at the nano-scale through conventional mixing: Van der Waals forces and nano-particles high surface areas cause aggregation in large clusters (Fig. 9), which prevents efficient transfer of nano-materials properties to the composite.

This topic is currently under investigation, being nano-particles available since the last few years, and the technique to obtain a homogeneous dispersion remains an open point. The most explored strategy is based on sonochemistry, the research area in which molecules undergo chemical reaction due to the application of powerful ultrasound radiation (20 kHz–10 MHz). The physical phenomenon responsible for sonochemical reaction is cavitation: creation, growth and explosion of bubbles that can decrease intermolecular forces and chemical bonds [19].

In order to test the effect of sonication on HTPB loaded with 1% of nAl, different samples of the same formulation,

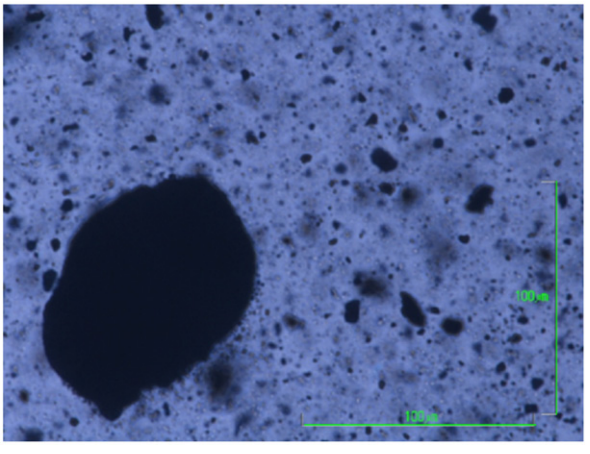

Fig. 9. HTPB loaded with 1% nAl (100 nm) and 0.2% C. Optical microscope, magnification 50 ×: evidence of big cluster formation.

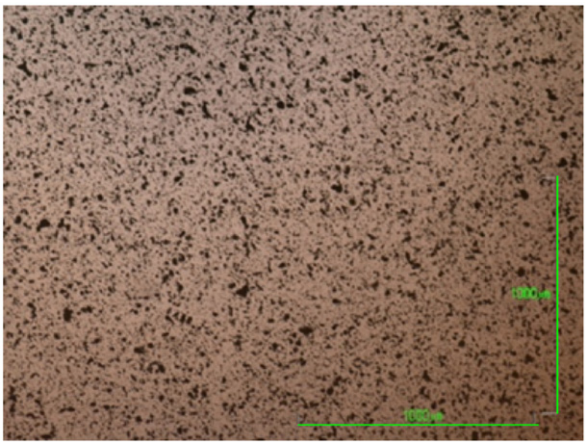

Fig. 10. HTPB loaded with 1% μAl (30 μm) and 0.2% C. Optical microscope, magnification 5 ×.

Table 8
Sum up of the formulations tested.

Formulation	Matrix	Filler	Sonication time
1	HTPB	1% μAl + 0.2% C	–
2	HTPB	1% nAl + 0.2% C	9
3	HTPB	1% nAl	30′
4	HTPB	1% nAl + 0.2% C	30′
5	HTPB	1% nAl + 0.2% C	60′

but obtained with different procedure were produced. Moreover, a comparison with a formulation loaded with 1% of μAl was carried out. As shown in Fig. 10, micrometric powders do not suffer from aggregation problems. The main differences in the preparations are underlined in Table 8.

A set of techniques to verify the degree of dispersion was selected; among them, the connection between mechanical properties of filled rubber and particles dispersion was considered. Optical microscope is also useful to identify big clusters presence. As shown in Fig. 11, aggregates are visible even at small magnification.

Microscope visualizations show that sonicated preparations have smaller agglomerates and dispersion is more uniform with respect to not sonicated ones. Samples sonicated for one hour are similar to samples sonicated for half an hour.

In order to verify dispersion properties of the samples, an indirect strategy is used, based on the connection between mechanical properties and dispersion [15,20]. In particular filler aggregates reduce elongation and maximum stress. Tensile stress–strain tests were carried out on dog-bones obtained from each formulations, stretching the samples at constant rate (50 mm/min). Results are shown in Fig. 12.

Sonicated samples have higher extensibility with respect to not sonicated ones. In particular half an hour of sonication offers better results with respect to 1 h of sonication. C improves extensibility of sonicated samples. Formulations loaded with μAl present the highest

Please cite this article as: L.T. DeLuca, et al., Characterization of HTPB-based solid fuel formulations: Performance, mechanical properties, and pollution, Acta Astronautica (2012), http://dx.doi.org/10.1016/j.actaastro.2012.05.002

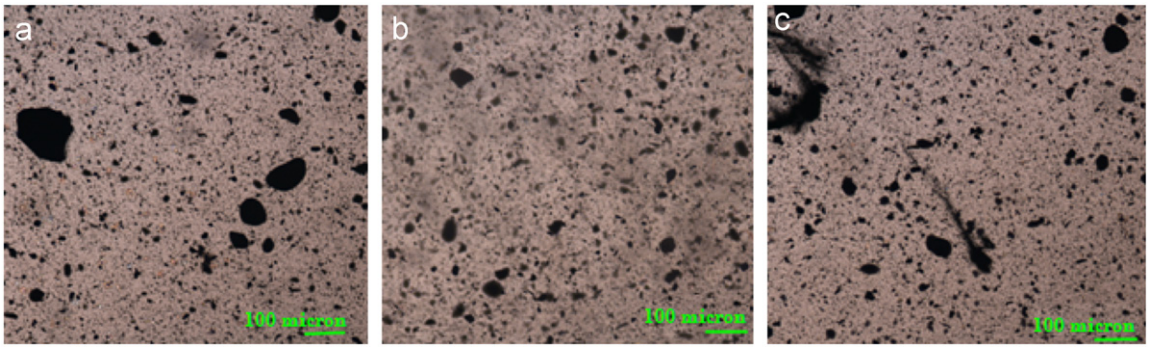

Fig. 11. HTPB loaded with 1% nAl and 0.2% C. Sonication effect on dispersion: (a) no sonic (b) 1/2 h sonic. (c) 1 h sonic. Optical microscope, magnification 10 ×.

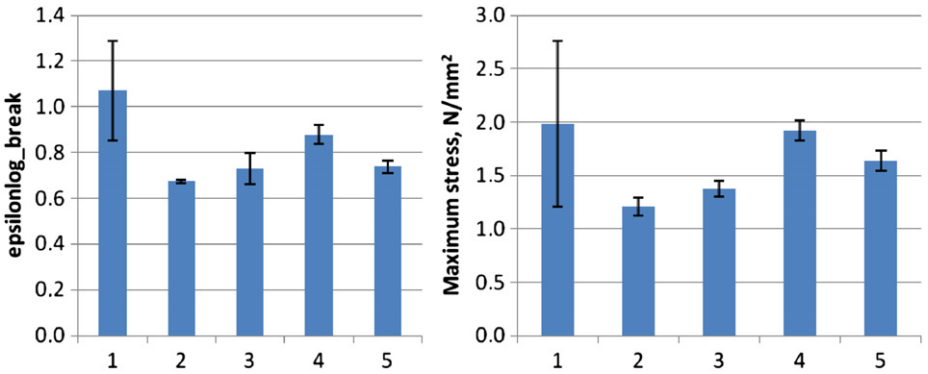

Fig. 12. Elongation and maximum stress of HTPB loaded with 1% μAl and 0.2% carbon black or 1% of nAl with and without carbon black. Sonication effect.

extensibility, since they do not suffer from aggregation problems.

Similar consideration can be done on maximum stress: higher values are given by sonicated samples, in particular when C is present. 1 h sonication improves maximum stress, but not with respect to samples sonicated for half an hour. Also for maximum stress, the highest value is offered by formulations containing μAl.

Results obtained in this investigation suggest that sonication improves dispersion, but too long sonication time can act in opposite direction increasing the possibility of particles contact [19]. C can act improving dispersion, but deeper investigations are needed in this area.

5. Environmental impact: pollution and climate change

Previous works and a specific AGARD workshop dealt with pollution concerns due to launch activity. Workshop conclusions suggested that minimal impact on the environment could be attributed to space-related human activities. Nevertheless, these optimistic conclusions were based on statistical data available in the mid 90 s, which comprised few tens of flights per year in the entire World [21]. If the current commercial forecasts are matched, in few years space tourism market will require about one thousand of flights per year and pollution level is doomed to rise. Among the others, hybrid rockets are specifically placed under the spotlight because, by now, they seem to represent the most suitable technology for private human space access.

A paper has recently been published by Ross et al. [3] on potential climate changes when hybrid rockets will daily flight from tourist spaceports. According to Ross' paper, this may represent a threat for global climate equilibrium since rocket motors emit more carbon black per unit mass propellant than aircrafts. Moreover, lifetime of pollution generated by rocket exhaust has been estimated to be longer because of direct release in the upper stratosphere from fixed locations (differently from aircraft pollution). Thus, "a fleet of 1000 launches per year of suborbital rockets would create a persistent layer of black carbon particles in the northern stratosphere that could cause potentially significant changes in the global atmospheric circulation and distributions of ozone and temperature" [3]. The discussion was concentrated on alterations of atmosphere radiative forcing due to C emission. Radiative forcing is a parameter which determines how human activities alter Earth energy balance. The average radiation of the Earth by the sun amounts to 342 W/m^2. A fraction (69%) of this energy is absorbed by the Earth and the atmosphere, and must be re-radiated back to the space for a correct energy balance [22]. Concentration rise of greenhouse gases and other pollutants, such as carbon black, act on radiative absorption and emission coefficients of the atmosphere and change radiative forcing parameter because it efficiently absorbs

Please cite this article as: L.T. DeLuca, et al., Characterization of HTPB-based solid fuel formulations: Performance, mechanical properties, and pollution, Acta Astronautica (2012), http://dx.doi.org/10.1016/j.actaastro.2012.05.002

solar shortwave radiation [23]. According to Ross' paper "after one decade of continuous launches, globally averaged radiative forcing from the black carbon would exceed the forcing from the emitted CO_2 by a factor of about 10^5 and would be comparable to the radiative forcing estimated from current subsonic aviation" [3].

Ross predictions are based essentially on Whole Atmosphere Community Climate Model, Version 3 (WACCM3), a comprehensive representation of atmospheric dynamics, ranging from chemistry to dynamics and radiative coupling. For the details of the specific simulation, readers are invited to consult the referenced paper [3]. Radiative forcing from carbon black rocket emission was estimated to be linearly dependent on the source emission index EI_{BC}. As a starting point, Ross assumed the emission index of N_2O/HTPB hybrid rockets as 60 g per kg of propellant consumed, sensibly larger than the index for LOX/RP1 liquid rockets set to 20–40 g/kg due to lower carbon particulate oxidation rate in the hot plume. This represents the crucial point for global impact evaluation.

Consideration on plume oxidation may be misleading. In fact, soot formation and destruction are complex kinetic processes that start in the combustion chamber where Polycyclic Aromatic Hydrocarbons (PAH) are generated, conglomerate into larger groups, grow, and finally are consumed by oxidizing species such as O, O_2 and OH. PAH are always present in nonpremixed flames, and so they are in a hybrid rocket. Soot precursors are usually formed in fuel rich environments within a specific temperature range (1000–2000 K), conditions commonly found close to the surface of a burning fuel grain, below the thin flame layer, as visible from Fig. 13. Moreover, a fraction of oxidizer may be still unreacted at the grain outflow and in fact hybrid rockets have a post-combustion chamber where mixing and residence time are enhanced.

Soot formation and destruction are kinetically driven and may depend on specific rocket design. Whereas thermodynamics would suggest that the limit for soot formation is when the ratio of carbon and oxygen atoms in the mixture is beyond the unity, the actual limit is below this value, falling down to about 0.45–0.50 for some premixed flames. However, thermodynamic computations may suggest behavior trends of different potential oxidizers such as O_2, N_2O, H_2O_2 and N_2O_4 (see Fig. 14). Computations are performed for combustion pressure of 30 bar; expansion ratio is set to 10. Carbon concentrations are expressed as grams per 100 g of propellant and are recorded at the nozzle throat, following the suggestion of a previous paper on rocket exhaust pollution [25].

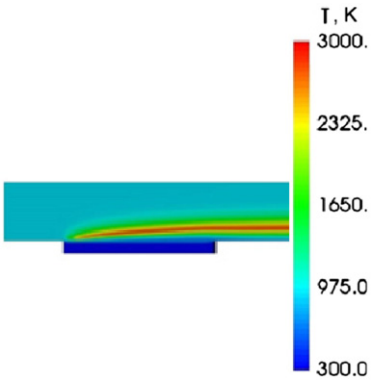

Fig. 13. Temperature field for a hybrid HTPB-O_2 flame. Image adapted from [24].

Notwithstanding the lack of a kinetic model, we may compare O/F for the value of C/O=1 (thermodynamic onset of soot production) with respect to O/F for maximum specific impulse. Considering O_2 and H_2O_2, the C/O ratio is close to unity when O/F is also close to one. Nevertheless, conditions for maximum specific impulse are quite different and set to around 2 for O_2 and about 6 for H_2O_2, very far from carbon production onset. According to these data, it appears that H_2O_2 is less prone to soot production. When N_2O is considered, C/O=1 is obtained for O/F around 3 while the maximum specific impulse is reached for O/F about 7.

Finally, the amount of soot produced depends on the O/F value. When hybrid rockets operate close to the maximum specific impulse, ideal thermochemistry predicts zero production of carbon black but as fuel rich mixtures are considered soot appears in the list of predicted exhaust products. In this case, the same order of magnitude of carbon as assumed by Ross may be found, yet far from the best operating conditions. Anyway, metals and organometallic compounds are known to decrease soot formation [26] as well as turbulence and electrical fields. Overall, soot emission from hybrid rockets is much complicated by their (i) peculiar flame structure, (ii) the fact that their operating conditions are continuously changing in time, and (iii) their little known exhaust plume afterburning processes in the upper atmosphere. Thus, a reliable prediction of soot emission by hybrid rockets, traversing in particular the stratosphere, is really perplexing without a systematic experimentation.

6. Conclusions and future work

HTPB, while offering good mechanical properties, suffers from low regression rates. Blending with paraffins does not help. In addition, the measured instantaneous quasi-steady rates do not obey the standard constant power law commonly used in the competent literature, even more so the time-average rates often reported by experimenters. How transient regression rates are affected remains to be seen. Another crucial matter to be properly investigated is soot formation.

A recommended strategy for HTPB-based solid fuels is to increase regression rates by fluid dynamics means (swirling flows); high-energy metallic additives can be used to sensibly increase density and specific impulse while contrasting nozzle erosion [2] and further augmenting regression rates [17]. With a suitable energetic ingredient addition, performance of HTPB-based hybrid rockets can reach levels neatly superior to the well-known RP1/LOX liquid couple (see Fig. 15). In this respect, AlH_3 appears the most promising fuel, as already discussed in [27] for example, offering a competitive edge to hybrid rocket propulsion for a variety of missions. A full discussion in this area was given by Calabro et al. [28].

Please cite this article as: L.T. DeLuca, et al., Characterization of HTPB-based solid fuel formulations: Performance, mechanical properties, and pollution, Acta Astronautica (2012), http://dx.doi.org/10.1016/j.actaastro.2012.05.002

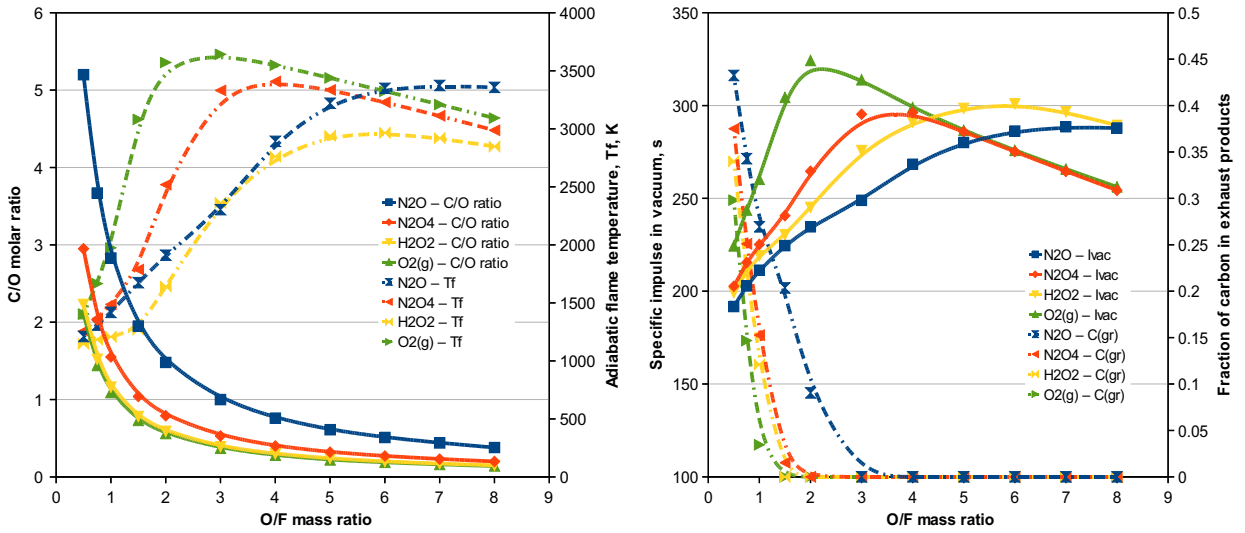

Fig. 14. Carbon-to-Oxygen ratio and adiabatic flame temperature (left) and specific impulse and carbon concentration (right) for different oxidizers burning with HTPB fuel. Pressure 30 bar, expansion ratio 10.

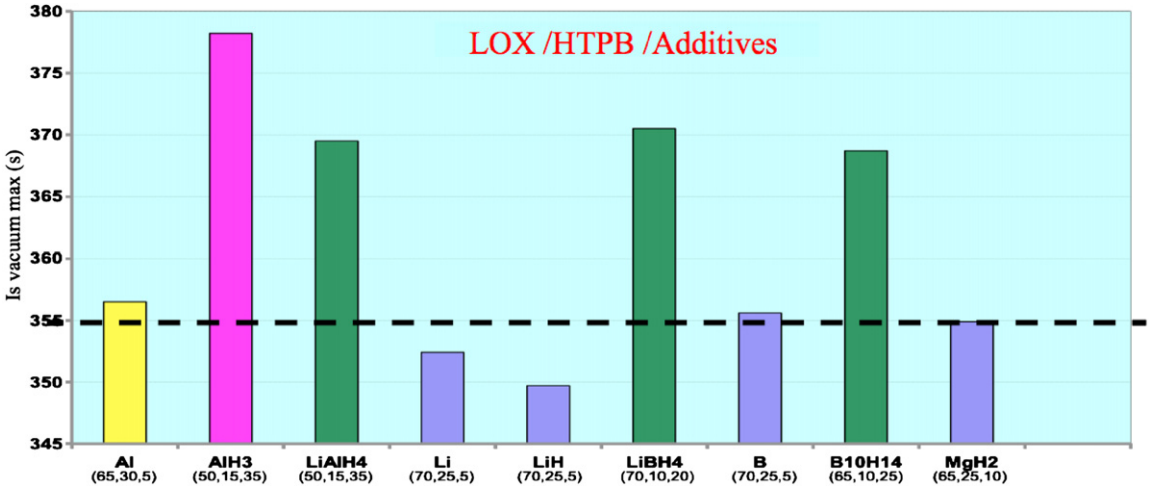

Fig. 15. Vacuum specific impulse of LOX/HTPB hybrid system as augmented by energetic additives. The reference dashed line corresponds to LOX/RP1 liquid bipropellant. [Courtesy of Calabro et al., 2007].

Users wish a suitable set of general properties regarding performance, combustion efficiency and stability, mechanical properties, handling safety, cost, environmental respect, commercial availability, chemical compatibility, etc. Only problems regarding filler dispersion, mechanical properties and exhaust pollution were discussed in this paper. Disturbing phenomena of 2-phase flow including fragmentation, aggregation/agglomeration, condensed combustion products were already shown in [29].

Acknowledgments

The authors wish to thank Mr. A. Adami, G. Massini, G. Rambaldi, and E. Seletti for providing a number of experimental data and useful discussions. This work was partially supported by CNES (Center National d'Études Spatiales) Launchers Directorate under contract nos. 4700024752/DLA090 and 4700028003/DLA094.

References

[1] V. Ziliotto, Relevance of the futron/zogby survey conclusions to the Current space tourism industry, Acta Astronaut. 66 (11–12) (2010) 1547–1552.
[2] D. Altman, Highlights in Hybrid Rocket Propulsion, in: L.T. DeLuca (Ed.), Proceedings of the 8th International Workshop on Combustion and Propulsion—IWCP, 2002.
[3] M. Ross, M. Mills, D. Toohey, Potential Climate Impact of Black Carbon Emitted by Rockets, Geophys. Res. Lett., 37, L24810, http://dx.doi.org/10.1029/2010GL044548.
[4] L.T. DeLuca, L. Galfetti, F. Bosisio, H. Raina, F. Maggi, G. Colombo, An Hybrid Microcombustor for Regression Rate Measurements, IAC-06-C4.2.01, in: Proceedings of the 57th International Astronautical Congress—IAC, Valencia, Spain, 2–6 October 2006.
[5] L. Galfetti, L.T. DeLuca, P. Grassi, C. Paravan, V. Luoni, A. Bandera, G. Colombo, L. DeCillia, R. Sempio, H. Raina, "Combustion Behavior

Investigation of Solid Fuels Using a Micro-sized Hybrid Rocket Motor", in: Kenneth K. Kuo, Hori Keiichi (Eds.), Advancements in Energetic Materials and Chemical Propulsion, Begell House, 2008.
[6] C. Paravan, M. Viscardi, A. Kazakov, L.T. DeLuca, Regression Rates and Anisotropy Effects in Hybrid Fuels Burning in a Micro-burner, in: Proceedings of the 3rd EUCASS Meeting, Versailles, Paris, France, 6–10 July 2009.
[7] L.T. De Luca, L. Galfetti, G. Colombo, F. Maggi, A. Bandera, M. Boiocchi, G. Gariani, L. Merotto, C. Paravan, A. Reina, Time-Resolved Burning of Solid Fuels for Hybrid Rocket Propulsion, in: Progress in Propulsion Physics, Torus Press, Moscow, vol. 2, 2011, pp. 405–426.
[8] T.J. Ohlemiller, M. Summerfield, A critical analysis of arc image ignition of solid propellants, AIAA J. 6 (5) (1968) 878–886.
[9] M.J. Chiaverini, Review of Solid Fuel Regression Rate Behavior in Classical and Nonclassical Hybrid Rocket Motors, in: M.J. Chiaverini, K.K. Kuo (Eds.), Fundamentals of Hybrid Rocket Combustion and Propulsion, AIAA Progress in Astronautics and Aeronautics, vol. 218, 2007, pp. 37–125 (Chapter 2).
[10] M.A. Karabeyoglu, Thermal Transients in Hybrid Rocket Solid Fuel Grains—Nonlinear Effects, AIAA Paper, 2007, p. 5369.
[11] F.P. Incropera, D.P. DeWitt, "Fundamentals of Heat and Mass Transfer", third ed. Wiley, New York, 1990.
[12] B. Evans, N.A. Favorito, K.K. Kuo, Study of Solid Fuel Burning Rate Enhancement Behavior in an X-ray Translucent Hybrid Rocket Motor, AIAA Paper 2005, p. 3909.
[13] G.A. Marxman, M. Gilbert, , Turbulent Boundary Layer Combustion in the Hybrid Rocket, in: Ninth International Symposium on Combustion, Academic Press, Inc., New York, 1963, pp. 371–383.
[14] M. Manzoni, G. Massini, C. Galbiati, C. Paravan, P. Tadini, A.A. Gromov, L.T. DeLuca, Pressure Dependence of HTPB- and Paraffin-based Solid Fuels for Hybrid Rocket Propulsion, in: proceedings of the 7th Perseus Seminar, CNES, Massy-Palaiseau, 02–03 February 12.
[15] L.E. Nielsen, "Mechanical Properties of Polymers and Composites", Marcel Dekker, Inc., New York, 1974.
[16] P. George, S. Krishnan, P.M. Varkey, M. Ravindran, L. Ramachandran, Fuel regression rate in hydroxyl-terminated polybutadiene/gaseous-oxygen hybrid rocket motors, J. Propul. Power 17 (1) (2001) 35–42.
[17] G.A. Risha, B.J. Evans, E. Boyer, R.B. Wehrman, K.K. Kuo, Nano-sized Aluminum and Boron-Based Solid Fuel Characterization in a Hybrid Rocket Engine, AIAA Paper, 2003, p. 4593.
[18] E. Duranti, A. Sossi, N.G. Rodkevich, A.B. Vorozhtsov, M.I. Lerner, A.A. Gromov, C. Paravan, L.T. DeLuca, Comparison Between Nano-sized Aluminum Powders with Different Coatings: Physical Analyses and Performance Test, HEM's 10: Demilitarization, Antiterrorism and Civil Application, Biysk-Naukograd (Russia), 8–10 September 2010.
[19] A. Gedanken, Doping nanoparticles into polymers and ceramics using ultrasound radiation, Ultrasonics Sonochemistry 14 (4) (2007) 418–430.
[20] A.R. Payne, Effect of dispersion on the dynamic properties of filler-loaded rubbers, J. Appl. Poly. Sci. 9 (6) (1965) 2273–2284.
[21] C.W. Hawks, Environmental Effects of Solid Rocket Propellants, Perceptions and Realities. In Environmental Aspects of Rocket and Gun Propellants, volume AGARD-CP-559 of AGARD Conference Proceedings, NATO, 1995.
[22] J. Warnatz, et al., Combustion, fourth ed. Springer, 2006.
[23] H. Nojoumi, I. Dincer, G.F. Naterer, Greenhouse gas emissions assessment of hydrogen and kerosene-fueled aircraft propulsion, Int. J. Hydrogen Energy 34 (3) (2009) 1363–1369, http://dx.doi.org/10.1016/j.ijhydene.2008.11.017.
[24] G. Gariani, F. Maggi, L. Galfetti, Numerical simulation of HTPB combustion in a 2D hybrid slab combustor, Acta Astronaut., 69(5–6):289-296, 10.1016/j.actaastro. 2011.03.015, 2011.
[25] P. Tishin, E.L. Alexandrov, The Impact of Space Launchers on the Earth Ozone Layer, Environmental Aspects of Rocket and Gun Propellants, volume AGARD-CP-559 of AGARD Conference Proceedings, NATO, 1995.
[26] I. Glassman, R.A. Yetter, Combustion, fourth ed. Academic Press, 2008.
[27] L.T. DeLuca, L. Galfetti, F. Severini, L. Rossettini, L. Meda, G. Marra, B. D'Andrea, V. Weiser, M. Calabro, A.B. Vorozhtsov, A.A. Glazunov, G.J. Pavlovets, Physical and Ballistic Characterization of AlH_3-Based Space Propellants, Aerospace Sci. Technol. 11(1): pp. 18–25, doi:10.1016/j.ast.2006.08.010, 2007.
[28] M. Calabro, L.T. DeLuca, L. Galfetti, C. Perut, Advanced Hybrid Solid Fuels, IAC-07-C4.2.09, in: Proceedings of the 58th International Astronautical Congress, Hyderabad, India, 2007.
[29] L.T. DeLuca, C. Paravan, A. Reina, E. Marchesi, F. Maggi, A. Bandera, G. Colombo, B.M. Kosowski, Aggregation and Incipient Agglomeration in Metallized Solid Propellants and Solid Fuels for Rocket Propulsion, AIAA Paper, 2010, p. 6752.

Please cite this article as: L.T. DeLuca, et al., Characterization of HTPB-based solid fuel formulations: Performance, mechanical properties, and pollution, Acta Astronautica (2012), http://dx.doi.org/10.1016/j.actaastro.2012.05.002